Histol Histopathol (2005) 20: 107-117

http://www.hh.um.es

Histology and Histopathology

Cellular and Molecular Biology

Changes in extranucleolar transcription during actinomycin D-induced apoptosis

A. Fraschini[1], M.G. Bottone[1], A.I. Scovassi[2], M. Denegri[2], M.C. Risueño[3], P.S. Testillano[3], T.E. Martin[4], M. Biggiogera[1,2] and C. Pellicciari[1,2]

[1]Dipartimento di Biologia Animale, Laboratorio di Biologia Cellulare e Neurobiologia, Università di Pavia, Italy, [2]Istituto di Genetica Molecolare CNR, Pavia, Italy, [3]Centro de Investigaciones Biológicas CSIC, Madrid, Spain and [4]Department of Molecular Genetics and Cell Biology, University of Chicago, IL/USA

Summary. Actinomycin D (AMD) inhibits DNA-dependent RNA polymerases and its selectivity depends on the concentration used; at very high concentrations it may also induce apoptosis. This study investigates the effects of different concentrations (0.01 to 1 μg/ml) of AMD on RNA transcription and maturation and on the organization of nuclear ribonucleoproteins (RNPs), and their relationship with apoptosis induction. Human HeLa cells were used as a model system. At the lowest concentration used, AMD induced the segregation of the nucleolar components and impaired r-RNA synthesis, as revealed by the decreased immunopositivity for bromo-uridine incorporation and for DNA/RNA hybrid molecules. The synthesis of pre-mRNAs, on the contrary, was active, while the immunolabeling of snRNP proteins and of the SC-35 splicing factor strongly decreased on perichromatin fibrils (where they are involved in co-transcriptional splicing). This suggests that the post-transcriptional maturation of extranucleolar RNAs was also affected. Moreover, still in the absence of typical late morphological or biochemical signs of apoptosis (i.e. chromatin condensation), these cells displayed the early apoptotic features, i.e. the externalization of phosphatidylserine residues on the plasma membrane and propidium iodide exclusion in vivo. At the highest concentrations of AMD used, apoptosis massively occurred, with the typical morphological events (progressive chromatin condensation, clustering of snRNPs and SC-35 splicing factor, cell blebbing). However, transcription of hnRNAs was maintained in the residual areas of diffuse chromatin up to advanced apoptotic stages. The inhibition of rRNA synthesis and the defective pre-mRNA maturation seem to be part of the apoptotic process induced by AMD.

Offprint requests to: Annunzia Fraschini, Dipartimento di Biologia Animale, Laboratorio di Biologia Cellulare e Neurobiologia, Università di Pavia, Piazza Botta 10, 27100 Pavia, Italy. Fax: +39 0382 9836 325. e-mail: nunziaf@unipv.it

Key words: Actinomycin D, RNA transcription and processing, Apoptosis, HeLa cells, Cytochemistry

Introduction

Actinomycin D (AMD) is an antibiotic which is able to bind DNA duplexes and to inhibit DNA-dependent RNA polymerases (Chen, 1988; Puvion-Dutilleul et al., 1992). At low concentrations (0.04-0.05 μg/ml), AMD specifically inhibits r-RNA synthesis in cultured cells, consistent with its selectivity for GC bases; at high concentration, however, AMD also affects the synthesis of other RNAs (Perry and Kelley, 1968; Peter et al., 1999). Under these conditions, apoptosis can also be induced in several cell lines (i.e. HL-60 human leukemic cells: Martin et al., 1990; Naora et al., 1996). In fact, defective, altered or arrested transcription may potentiate apoptosis even in normal and tumor cell lines, which are usually resistant to cell death induced by several agents (i.e. DNA-damaging agents: Martin, 1993; Andera and Wasylyk, 1997; Peter et al., 1999).

The aim of the present study was to investigate the behaviour of the extranucleolar RNA (hnRNA or pre-mRNA) synthesis and of its maturation process in AMD-induced apoptosis.

In the nucleus, RNA transcription and transcripts' maturation occur in specific structures which have been described, at electron microscopy, as perichromatin fibrils (PF), perichromatin granules (PG), and interchromatin granules (IG) (Fakan, 1994, 2004; Spector, 1996). In particular, PF are the morphological equivalent of hnRNA transcription and co-transcriptional splicing, while IG represent a storage site for snRNP and non-snRNP splicing factors and are a possible site for spliceosome assembly (Misteli and Spector, 1998; Melcak et al., 2001). Finally, PG are involved in the storage and the nucleus-to-cytoplasm transport of mRNA (Fakan, 1994, 2004). All these

components have specific intranuclear location (PF and PG, at the periphery of condensed chromatin; IG, in the so-called interchromatin space), which is an essential pre-requisite for the correct maturation of nuclear RNAs (for reviews, see Puvion and Puvion-Dutilleul, 1996; Fakan, 2004).

In the present investigation, different concentrations of AMD were used in the attempt to monitor the changes in nucleolar and extranucleolar RNA synthesis and processing in relation to the occurrence of apoptosis. HeLa cells have been selected as a model cell system, and immunocytochemical techniques, at light and electron microscopy, have been mainly used to label the sites of pre-mRNA synthesis, and to detect the incorporation of RNA precursors and the presence of DNA/RNA hybrid molecules. To follow the intranuclear locations of the post-synthetic RNA processing, some key proteins such as hnRNP, snRNP and the SC-35 splicing factor were immunolabeled. Cytometric and electrophoretic techniques have been used to detect the presence of apoptotic cells and to estimate their percentages.

Materials and methods

Cells, culture conditions and treatments

HeLa cells were grown in D-MEM Medium, containing 10% fetal bovine serum, 2 mM glutamine and 100 units each of streptomycin and penicillin (Celbio S.r.l., Milano, Italy). The cells were grown at 37 °C in a humified atmosphere containing 5% CO_2, and were grown either in 25 cm^2 flasks or planted on glass coverslips in Petri dishes.

$2x10^4$ cells/cm^2 were seeded and allowed to grow in culture for 48 hr; the cell cultures were then treated for 12 hr with AMD at different final concentrations (0.01, 0.1 or 1 µg/ml). The time of treatment was selected, based on preliminary experiments in which AMD exposure lasted for 30 min to 24 hr. Control cell samples were grown in complete fresh medium without AMD.

Cells were harvested by mild trypsinization (0.25% trypsin containing 0.05% EDTA in PBS) and processed for electron microscopy cytochemistry, fluorescence microscopy, cytofluorometry or the biochemical assays (see below).

Detection of RNA synthesis

^{3}H-Uridine Incorporation: Control and AMD-treated cell samples were incubated for 1 hr with 7 µCi of ^{3}H-uridine (Amersham, UK: specific activity 26 Ci/mMol). After removing the radioactive medium, cells were washed with PBS, and lysed with 1 ml of 1M NaOH for 10 min at 37 °C. Cell lysates were then transferred to 10 ml tubes, and nucleic acids were precipitated with 3 ml of cold 20% TCA. Radioactive material was recovered by precipitation under vacuum on GF/C filters, which were washed three times with cold 3% TCA, once with cold ethanol, and dried. Radioactivity was measured by liquid scintillation in a beta Counter Beckman LS 6000. Experiments were performed in triplicate.

Bromo-Uridine incorporation: Control and AMD-treated cells were incubated for 30 min. with 25mM bromo-uridine (BrU: Sigma Chemical Co., St. Louis, CA, USA.), as originally suggested for non isotopic precursors by Dundr and Raska (1993). Cells were then fixed in suspension with 70% ethanol, washed in PBS and incubated for 60 min at room temperature with a mouse monoclonal anti-bromodeoxyuridine (BrdU) antibody B44 (Becton-Dickinson, San José, CA, USA), which has affinity also for BrU, thus recognizing BrU-substituted RNA, without previous acid hydrolysis (Jensen et al., 1993). The anti-BrdU antibody was diluted 1:10 in PBS (containing 0.05% Tween 20 and 0.1% bovine serum albumin), then revealed with an FITC-conjugated goat anti-mouse antibody (Sigma Chemical Co). Cell samples were finally counterstained for at least 30 min at room temperature with 5 µg/ml propidium iodide (PI in 0.1 M phosphate buffer pH 7.2, containing 100 units/ml RNAse A from Sigma). Bivariate measurements of green fluorescence (identifying immunolabeled cells) versus red fluorescence (PI-DNA content) were made with a Becton Dickinson (San José, CA, USA) FACStar flow cytometer. This was carried out under the following conditions: argon ion laser excitation power 200 mW at 488 nm, 560 nm beam splitter, 510-540 nm band pass filter for the green fluorescence detector, and 610 nm long pass filter for the red fluorescence detector. The level of background fluorescence, due to the non-specific binding of the FITC-conjugated antibodies, was established using control cell specimens processed as described above, but either without incubation with the primary antibodies or with incubation with a mouse serum containing no specific antigenic activity: the corresponding value of green fluorescence was used as a cut-off value above which cells were considered as labeled. Dual parameter cytometric data were evaluated with rectangular region analysis: FITC-immunolabeled cells were those with green fluorescence values exceeding the background threshold determinated as reported above; the ranges for G_0-G_1, S and G_2-M phase cells were established on the basis of the corresponding DNA content histograms. At least 20,000 cells per sample were considered in the gated region used for calculations.

Detection of BrU incorporation, DNA/RNA hybrid molecules and RNPs at electron microscopy

For ultrastructural cytochemistry, the cells were fixed in suspension with 2% p-formaldehyde containing 0.2% glutaraldehyde in D-MEM medium for 1 h at 4 °C. The samples were then centrifuged and embedded in 2% agarose. Small fragments were dehydrated in ethanol and finally embedded in LRWhite resin. 60-70 nm thick

sections were cut and mounted on nickel grids.

The characteristics of the monoclonal and polyclonal antibodies used are listed in Table 1. After pre-incubation with normal goat serum (1:100 dilution in PBS, pH 7.4 for 3 min) the grids were incubated overnight with one of the primary antibodies diluted in PBS contaning 0.05% of Tween 20 and 0.1% of bovine serum albumin, then revealed by gold-conjugated secondary antibodies for 30 min; all incubations were performed at 23 °C.

Since the presence of BrU incorporated into pre-mRNA molecules can inhibit splicing (Wansink et al., 1994), the antibodies specific for proteins involved in splicing were used on cells cultured in the absence of BrU. As a control of the specificity of the reactions, some grids were processed in the absence of the primary antibody.

BrU incorporation was detected using the anti-BrdU B44 antibody (Becton-Dickinson), followed by the gold-conjugated goat-anti-mouse antibody (Jackson Immuno Research Laboratories, Pennsylvania, USA). As a specificity control for the labelling, the immunoreaction was also performed after digestion with RNase A (100 KU/ml at 37 °C for 2 hr).

DNA/RNA hybrid molecules were detected by a goat polyclonal antibody (Testillano et al., 1994), and revealed by a gold conjugated rabbit anti-goat antibody (Multilab, Fetcham, England).

To label *hnRNPs involved in hnRNAs processing*, the C8V chicken polyclonal antibody raised against hnRNP core proteins (Jones et al., 1980; Martin and Okamura, 1981; Leser et al., 1984) was used; the grids were then reacted with a rabbit anti-chicken antibody and finally visualized by gold-conjugated goat-anti-rabbit IgG (Multilab, Fetcham, England).

snRNPs labeling: Hybridoma supernatant containing the monoclonal antibody recognizing the Sm complex present on U1, U_2, U_2/U_6 and U-5 snRNP (Lerner et al., 1981) was used and then reacted with a goat-anti-human IgG coupled with gold particles (Aurion, Wageningen, The Netherlands).

The *non-snRNP splicing factor SC-35* was immunolabeled with the specific mouse monoclonal antibody (Fu and Maniatis, 1992) (Sigma Chemical Co.), then evidenced by gold-conjugated IgG+IgM (Multilab).

At the end of all the immunocytochemical procedures, the sections were stained with Bernhard's regressive EDTA method (Bernhard, 1969), in order to evidence the nuclear structures containing RNPs, such as PG and IG.

The sections were examined and photographed under a Zeiss TEM 900 at 80kV.

Fluorescence microscopy

Micrographs were obtained from cells grown on glass coverslips and immunoreacted to detect either BrU incorporation or SC-35 splicing factor, using FITC-conjugated secondary antibodies, in the same conditions as described above. Cells were then counterstained for DNA with 0.1 µg/ml Hoechst 33258 (Sigma Chemical Co.) in PBS for 15 min.

After the cytochemical procedures, slides were mounted in Mowiol 4-88 (Calbiochem, La Jolla, CA, USA) and observed with an Olympus BX 50 microscope equipped with a 100W mercury lamp. The following conditions were used: 330-385 nm excitation filter (excf), 400 nm dichroic mirror (dm) and 420 nm barrier filter (bf), for Hoechst; 450-480 nm excf, 500 nm dm and 515nm bf for FITC. The images were recorded with an Olympus Camedia C-2000 Z digital camera and stored for processing on a PC by the Olympus software.

Identification of apoptotic cells

Labeling of phosphatidylserine residues on the outer leaflet of the plasma membrane: Unfixed cells were incubated with FITC-conjugated annexin V (3 µl/10^6 cells, Bender MedSystem, Prodotti Gianni, Milano, Italy) and counterstained with 2 µg/ml PI. After 10 min of incubation, dual-parameter flow cytometric analysis was perfomed with a FACStar flow cytometer as reported above.

Phosphatidylserine residues were also labeled for electron microscopy, using biotin-conjugated Annexin V (3 µl/10^6 cells, Bender MedSystem). Cells were then fixed with 2% glutaraldehyde, dehydrated and embedded in LR White resin. Ultra-thin sections were reacted with a gold-conjugated goat anti-biotin antibody (Aurion, Wageningen, The Netherlands) 1:5 in PBS for 30 min at room temperature (Pellicciari et al., 1997). As a control for the reaction specificity, some sections were pre-treated with streptavidin to block biotin.

Detection of hnRNP proteins by Western blot

Table 1. Antibodies.

ANTIBODY	SOURCE	ANTIGEN	DILUTION	SECONDARY MARKER	REFERENCE
Anti-BrdU	mouse, monoclonal	Br-uridine	1:5	GAM IgG+IgM (12 nm)	Jensen et al., 1993
Anti-hybrid	goat, policlonal	DNA/RNA hybrids	1:100	RAG, 20 nm	Testillano et al., 1994
C8V	chicken, polyclonal	hnRNP core proteins	1:3000	Rabbit anti-chicken / GAR, 12 nm	Martin and Okamura, 1981
Anti-Sm	autoimmune serum	Sm antigen (U1, U2, U4/6, U5 snRNP)	1:200	GAHu, 12 nm	Lerner et al., 1981
SC-35	mouse, monoclonal	SC-35 non snRNP splicing factor	1:100	GAM IgG+IgM, 12 nm	Fu and Maniatis, 1992

analysis: Cells were washed twice with ice-cold PBS and resuspended at the concentration of $5x10^6$ cells/ml in denaturing buffer containing 62.5 mM Tris-HCl (pH 6.8), 4 M urea, 10% glycerol, 2% beta-mercaptoethanol and 0.003% bromophenol blue (Shah et al., 1995). Cells were then disrupted by sonication on ice, twice for 30 s at 60W. Equal volumes of each sample were incubated for 15 min at 65 °C before loading on SDS-polyacrylamide gel, electrophoresed in a 7.5% SDS-PAGE minigel and transferred by standard procedures to nitrocellulose filters (Biorad, Hercules, CA, USA). The membranes were saturated overnight with PBS containing 10% newborn calf serum and 0.2% Tween (PTN) and then incubated overnight with the chicken polyclonal antibody C8V against hnRNPs (Martin and Okamura, 1981), 1: 10000 in PTN. After washing with PBS containing 0.2% Tween 20, the membrane was incubated for 2 hr with the appropriate secondary antibody conjugated to horseradish peroxidase. Visualization of peptides was achieved by ECL system (NEN-Dupont, Boston, USA).

Results

Under control growth conditions, BrU incorporation takes place all over the nucleus, including the nucleoli which were strongly immunopositive (Fig. 1a). After 12 hr of treatment with 0.01 µg/ml of AMD (Fig. 1b), the nucleoli were unlabelled, whereas the extranucleolar nuclear areas were still immunopositive; it is worth noting that similar results were already obtained after 30 min of treatment with 0.01 µg/ml of AMD (not shown). After 12 hr of treatment with higher AMD concentrations (0.1-1 µg/ml: Fig. 1c,d), the extranucleolar labeling also decreased. The quantitative variations in BrU incorporation were apparent from the flow cytometric analyses as well as the experiments of ^{3}H-uridine incorporation (Fig. 2 and Table 2).

At the electron microscope, in control cells both the incorporation of BrU (Fig. 3a) and the presence of DNA/RNA hybrids (Fig. 4a) were found in the fibrillar component of the nucleolus and in the PF; such RNP-containing structures were preferentially stained with the EDTA regressive procedure. In cells treated with 0.01 µg/ml AMD, nucleoli underwent segregation and only a weak (or even absent) immunogold labeling for BrU (Fig. 3b) and for DNA/RNA hybrid molecules was observed (Fig. 4b); consistent with the immunofluorescent experiments, incorporation of BrU still occurred outside the nucleolus, in the PF, where DNA/RNA hybrid molecules were also detected; this suggests that pre-mRNA synthesis was still active. The hnRNP core proteins, which associate to newly synthesized pre-mRNA, were present on PF in control cells (Fig. 5a) and were still observed after AMD treatment (Fig. 5b).

In control cells, the protein components necessary for splicing, such as snRNPs (Fig. 6a) and the SC-35 splicing factor (Fig. 7a), were localized on the PF (where co-transcriptional splicing is also known to occur), and on the IG (which serve as storage sites for splicing proteins). At light microscopy, the immunopositivity for SC-35 in untreated cells was present in the nucleus either as fluorescent spots or as a diffuse pattern (Fig. 7a, inset).

After 0.01 µg/ml AMD, the immunolabeling of both snRNP (Fig. 6b) and the SC-35 splicing factor (Fig. 7b), at the electron microscope, strongly decreased on PF, while a residual positivity was present on the IG which appeared more clustered than in controls; consistently, at light microcopy the diffuse immunopositivity was highly reduced, whereas the fluorescent spots were still evident and increased in size (Fig. 7b, inset).

No significant changes in chromatin organization still occurred in cells treated for 12 hr with 0.01 µg/ml of AMD (Fig. 6b), although about 20% of the cells started to display phosphatidylserine residues at the surface of the plasma membrane (Fig. 6b, inset and Fig. 8): this is considered as a precocious sign of apoptosis (Fadok et al., 1992).

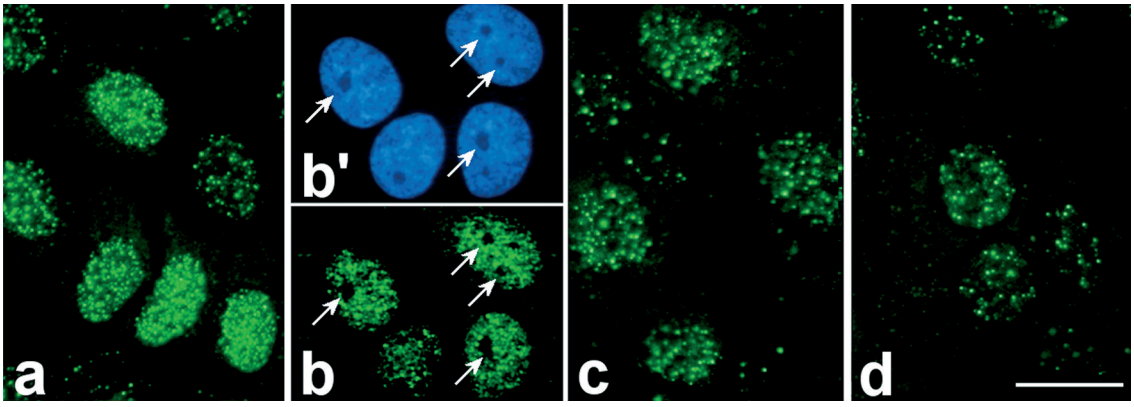

Fig. 1. Immunofluorescence patterns of BrU incorporation. As compared to control cells **(a),** in the cells treated with 0.01 µg/ml AMD **(b)** the nucleoli (arrows) were devoid of immunolabeling **(b')**, the same field as in **b**, after staining of DNA with Hoechst 33258: note that nucleoli are not stained). At higher AMD concentrations (**c**, 0.1 and **d**, 1 µg/ml) also the extranucleolar labeling progressively decreased. Bar: 20 µm.

After treatments with higher AMD concentrations (0.1 to 1 μg/ml), the percentage of apoptoptic cells dramatically increased, as demonstrated by the dual-parameter cytograms of annexin V-positivity versus PI staining (Fig. 13); these evidence was also confirmed by gel electrophoresis of low-molecular-weight DNA and of PARP-1 degradation (personal observation, not shown); interestingly enough, in these cells the extranucleolar pre-mRNA synthesis still remained active, although the incorporation of both BrU and ^{3}H-uridine progressively decreased (see Table 2). Even in cells which, after treatment with higher AMD concentrations, clearly exhibited morphological signs of apoptosis (i.e. chromatin condensation, cytoplasmic blebbing), BrU incorporation and DNA/RNA hybrid molecules were still associated with the EDTA-positive PF in the non-condensed chromatin regions (Fig. 9), always in association with residual immunolabeling for hnRNPs (Fig. 10). In these apoptotic cells, fibrogranular RNP-containing structures were observed in the residual areas of loosely dispesed chromatin: they contain different splicing proteins, such as snRNPs and the SC-35 splicing factor (Fig. 7c) and recall the heterogeneous nuclear structures which have been called HERDS (for Heterogeneous Ectopic RNP-derived Structures: Biggiogera et al., 1998) which originate from the segregation and the displacement of nucleolar and extra-nucleolar RNPs from their original nuclear sites. HERDS may move from the nucleus to the cytoplasm to be extruded from the cell in the late apoptotic stages: in fact, in our model system fluorescent aggregates immunoreactive for the SC-35 splicing factor were observed outside the nucleus of AMD-induced apoptotic HeLa cells (Fig. 7c, inset). It is worth noting that, in our experiments, hnRNP proteins were never observed to aggregate into these ectopic RNP clusters: this is in agreeement with the Western blot analyses (Fig. 11) which demonstrated that in control cells two main bands of 33 and 40 kDa were recognized by the antibody against hnRNP core-proteins, whereas after treatment with high concentrations of AMD the band with higher molecular weight disappeared; this suggests that hnRNPs are degraded in situ during apoptosis, whereas it is known that other RNP-containing antigens (such as the Sm antigen) are not degraded (Casiano et al., 1996; Biggiogera et al., 2004).

Discussion

Our data on HeLa cells confirm the reports in the literature on AMD inhibition of r-RNA synthesis: this was demonstrated both by absence of BrU incorporation and by the lack of labeling for DNA/RNA hybrid molecules in the nucleolus, a method used for the first time under these conditions. These events were paralleled by the segregation of nucleolar components,

Table 2. Quantitative study.

	CONTROL	AMD 0.01 μg/ml	AMD 0.1 μg/ml	AMD 1 μg/ml
BrU incorporation (immunofluorescence intensity)	182.0±2.3 (100%)	123.0±3.0 (67.0%)	82.4±3.1 (45.3%)	38.9±4.3 (21.4%)
^{3}H-Uridine incorporation (radioactivity)	1776±8.2 (100%)	899±10.9 (50.8%)	576±8.9 (32.6%)	144±1.4 (8.5%)

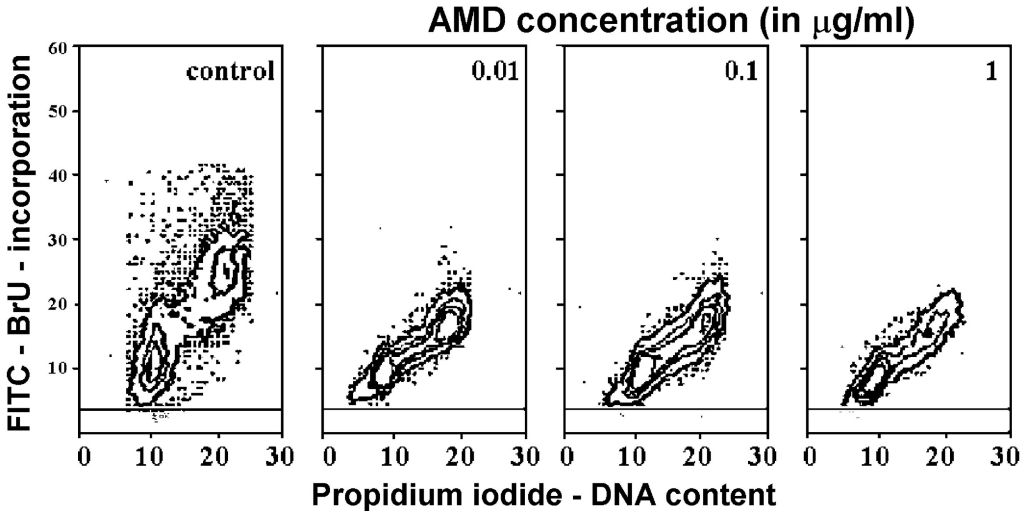

Fig. 2. Dual-parameter cytograms of BrU incorporation (FITC-immunolabeling, in ordinate), versus PI-DNA content (in abscissa). BrU incorporation progressively decreased with increasing AMD concentration. The horizontal line in each cytograms is for the FITC-fluorescence values of negative controls.

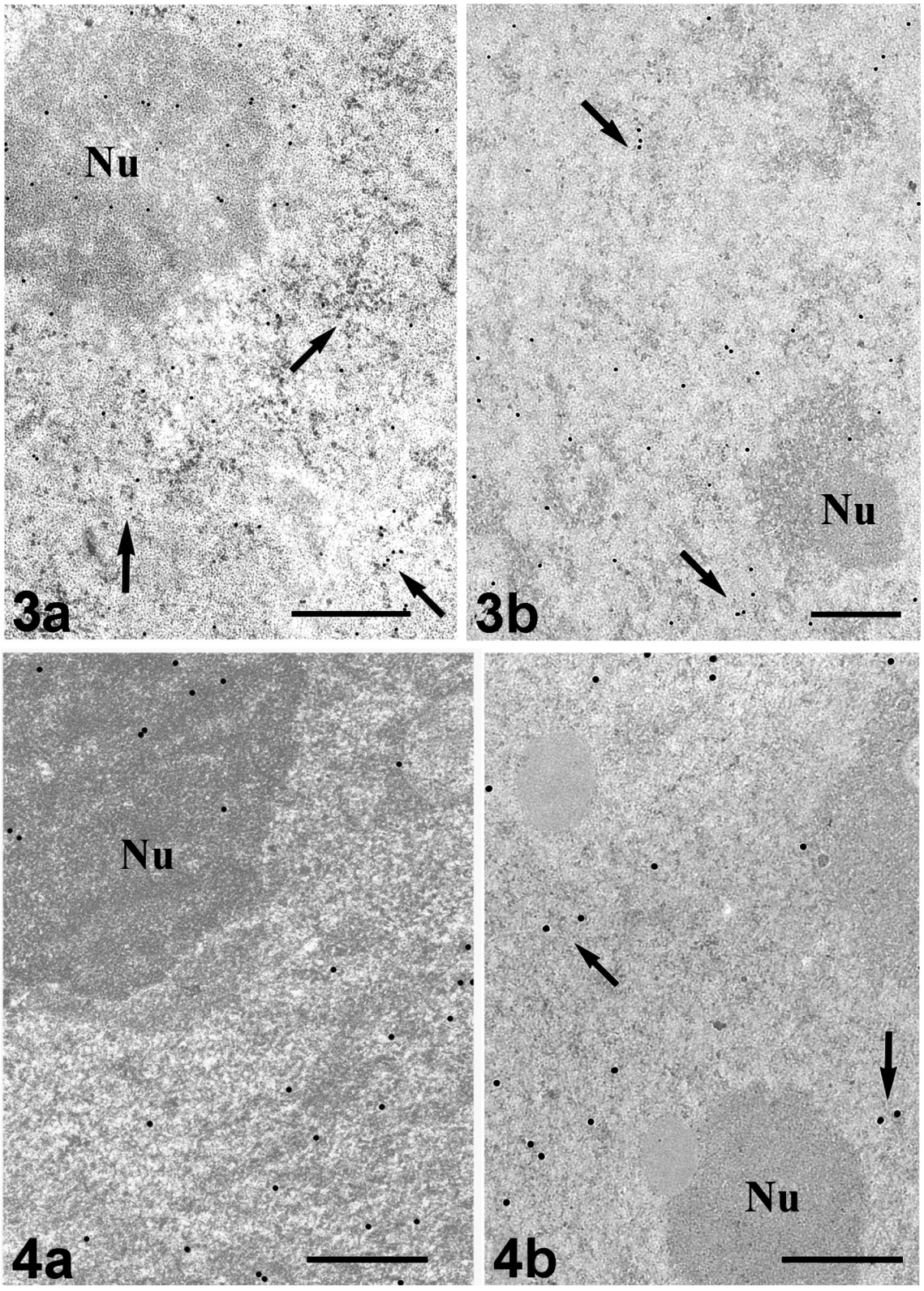

Fig. 3. Immunolabeling with anti-BrdU antibodies and EDTA regressive staining. In control cells **(a)**, the gold particles label the sites of BrU incorporation on the dense fibrillar component of the nucleolus (Nu) and on PF (arrows). After 0.01 AMD **(b)**, the segregated nucleolus (Nu) appears devoid of immunolabeling whereas PF (arrows) are still labeled. Bar: 0.5 µm.

Fig. 4. Strong immunolabeling for DNA/RNA hybrid molecules was observed all over the nucleus (including the nucleolus) in control cells **(a)**, whereas after 0.01 AMD treatment **(b)** DNA/RNA hybrid molecules are not immunodetectable in the segregated nucleolus (Nu), while they are still present on PF (arrows). Bar: 0.5 µm.

which is a typical structural sign of functional inactivation of the nucleolus (Puvion and Puvion-Dutilleul, 1996; Fakan, 2004).

On the contrary, the synthesis of pre-mRNAs still remained active (although gradually decreasing) for longer treatment times (up to 12 hr), as shown by the occurrence of BrU incorporation and by the presence of DNA/RNA hybrids on PF. However, the immunopositivity for snRNPs and SC-35 strongly decreased on PF, and the scanty residual labelling was mostly confined to IG: this decrease is considered as a hallmark of defective processing of the extranucleolar transcripts. In fact, PF are made of nascent hnRNAs (or pre-mRNAs), hnRNPs, snRNPs and the SC-35 splicing factor (Fakan et al., 1986; Spector et al., 1991; Fakan, 1994, 2004; Cmarko et al., 1999) and have been recognized as the morphological expression of extranucleolar transcription and co-transcriptional splicing. The residual splicing proteins in the nucleus, located in the IG, should be non-functional. Actually, IG represent storage sites of hypophosphorylated snRNPs and serine-arginine rich proteins, such as SC-35 (Fakan, 1994, 2004; Misteli and Spector, 1998): only after being activated by phosphorylation, they can be recruited from IG to PF (Caceres et al., 1997; Misteli and Spector, 1997). On the other hand, IG can also contain released transcripts which are believed to move from DNA the reservoirs of splicing factors (Melcak et al., 2000).

The overall decrease in the immunolabeling for these proteins after treatment with 0.01 µg/ml AMD could be ascribed either to an inhibition of their synthesis or to their storage inside IG which results in

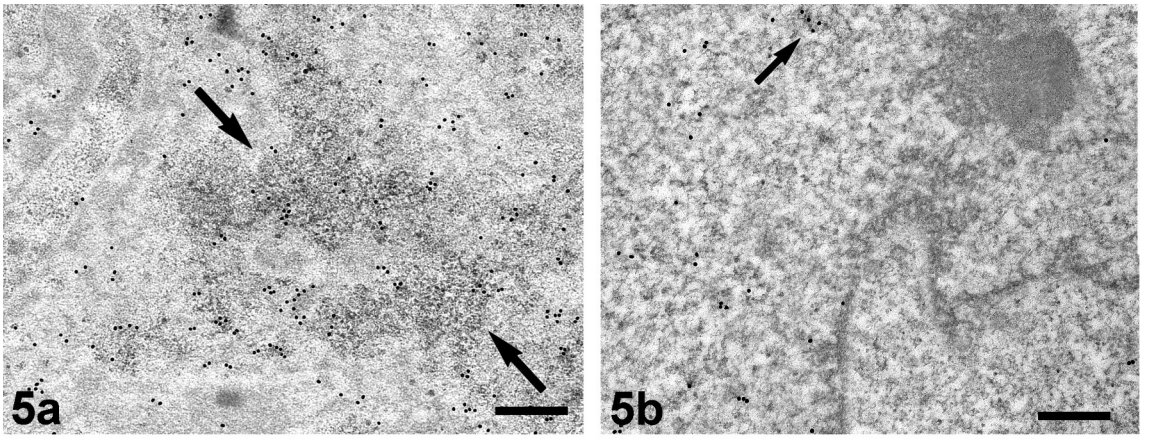

Fig. 5. Immunonogold labeling of hnRNP core proteins. In control cells **(a)**, the gold grains were exclusively located on PF (arrows), where hnRNP core proteins were still detectable after treatment with 0.01 mg/ml AMD **(b)**. Bar: 0.5 µm.

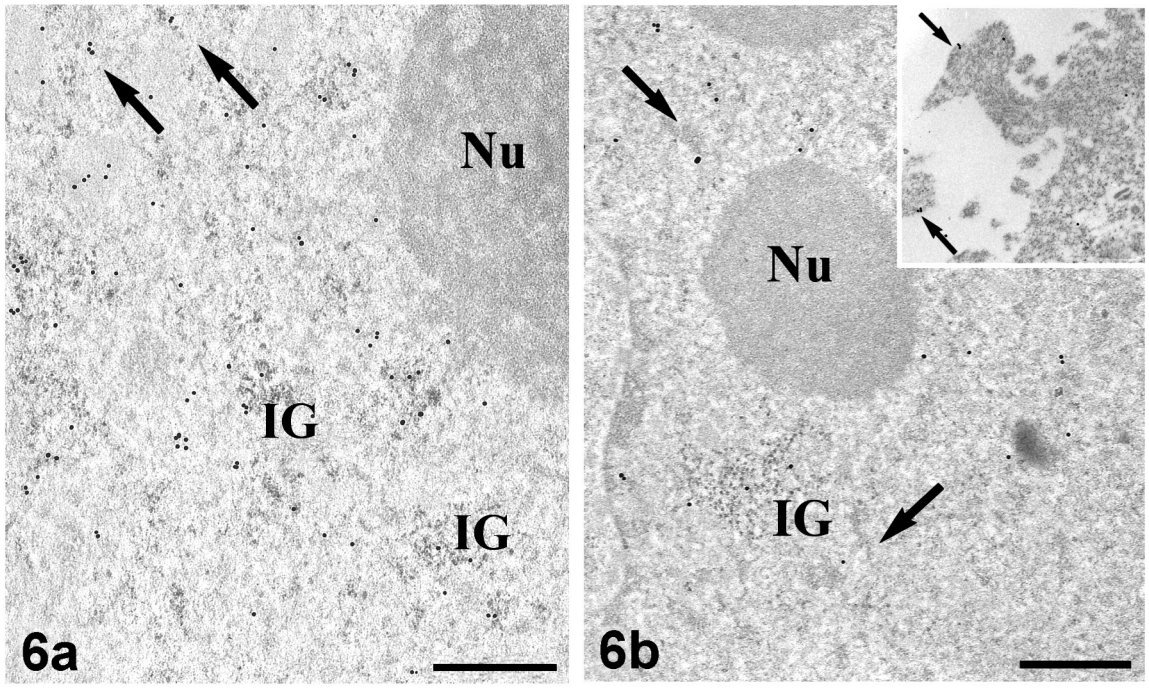

Fig. 6. Immunogold labeling for snRNP. In control cell **(a)**, PF (arrows) and IG were typically labeled, whereas after treatment with 0.01 mg/ml AMD, a rather scarce immunolabeling for snRNPs can be observed (Nu: nucleolus); after AMD treatment **(b)**, the labeling decreases mainly on PF (arrows), while IG are still labeled; in the micrograph, a segregated nucleolus (Nu) was observed. Inset: gold-labeling with Annexin V of the phosphatidylserine residues on the plasma membrane of a cell with segregated nucleolus (not shown). Bar: 0.5 µm.

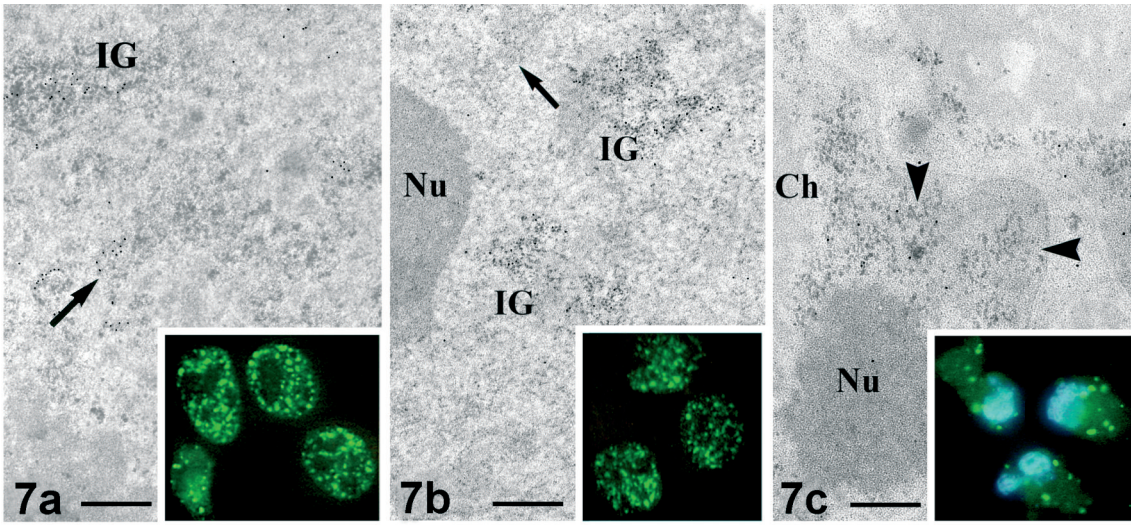

Fig. 7. Immunolabeling for the SC-35 splicing factor. In control cells, PF and IG were mainly labeled **(a)**; inset: FITC immunofluorescence of SC-35 is present either as "spots"or in a diffuse form. After 0.01 µg/ml AMD **(b)**, the labeling for SC-35 was mainly present on IG, whereas PF (arrow) were clearly less labeled; inset: the immunofluoresence appears only as "spots". Nu: nucleolus. After 0.1 µg/ml AMD treatment **(c)**, the SC-35 splicing factor can be detected in ectopic aggregates (arrowheads) which move from the nucleus to the cytoplasm in late apoptotic cells (inset). Bar: 0.5 µm.

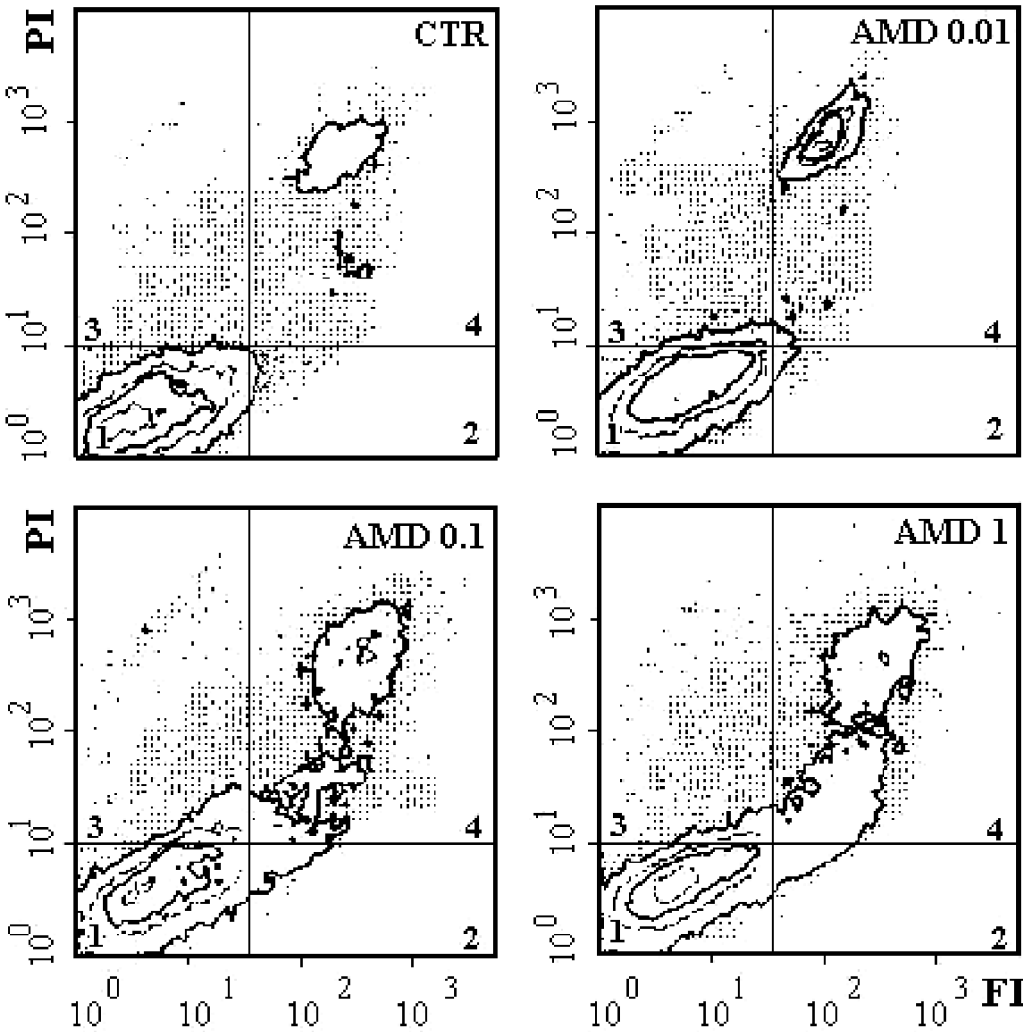

Fig. 8. Dual-parameter cytograms of FITC-conjugated Annexin V (in abscissa) versus propidium iodide (PI, in ordinate). In control cell cultures (CTR) almost all the events fell in quadrant 1, being negative for both Annexin V and PI; the few cells in quadrant 4 are spontaneously apoptotic cells, positive for both dyes. After 0.01 µg/ml of AMD, early apoptotic cells, which are positive for Annexin V (quadrant 2) but negative for PI (being their membrane still able to exclude PI) can be found, whereas at higher concentrations (0.1 and 1 µg/ml of AMD) a large number of late apoptotic cells (positive for both Annexin V and PI: quadrant 4) were present.

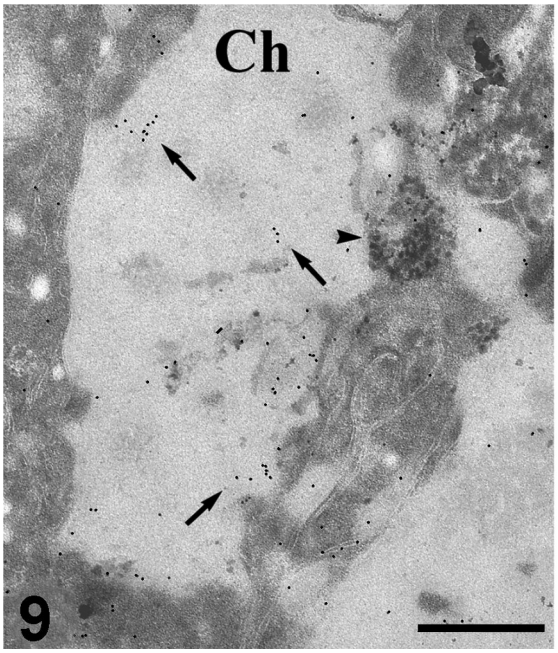

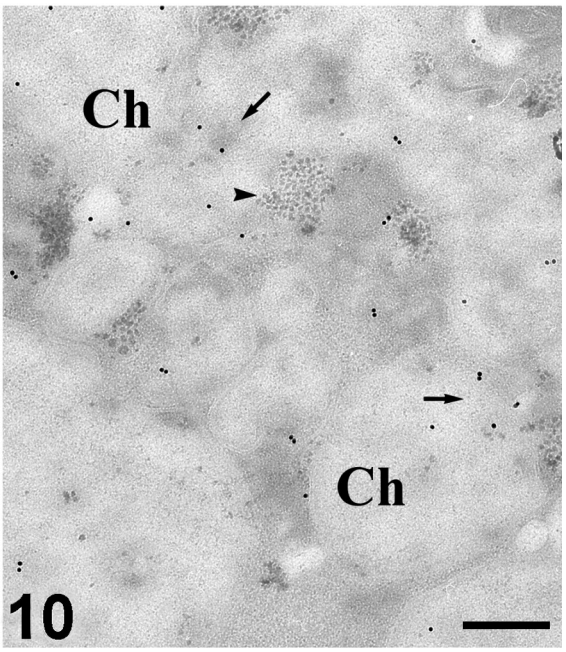

Fig. 9. BrU immunolabeling and regressive EDTA staining of HeLa cells after 0.1 µg/ml AMD treatment. Chromatin (Ch, bleached by this procedure) is extensively condensed. Few stained RNP structures still incorporate BrU (arrows). Bar: 0,5 µm.

Fig. 10. Immunogold labeling of hnRNP core proteins and regressive EDTA staining in a cell treated with 0.1 µg/ml of AMD. The hnRNPs are still present in EDTA-stained structures (arrows) inside the bleached chromatin (Ch).

Arrowheads point to ectopic aggregates, which are devoided of hnRNP. Bar: 0.5 µm.

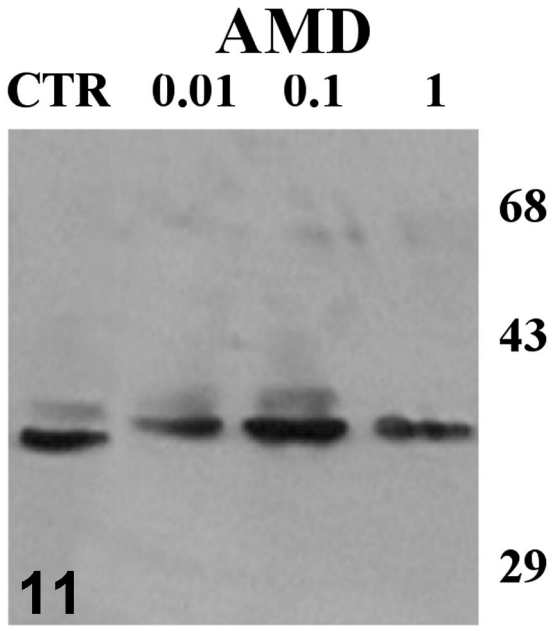

Fig. 11. Western blot of hnRNPs. In control cells (CTR), as well as in cells treated with 0.01 and 0.1 µg/ml of AMD, two bands are present. After treatment with 1 µg/ml of AMD, only one protein band is detectable, suggesting a partial degradation of the hnRNPs.

the clustering and, probably, masking of the epitope. In fact, degradation of these proteins is unlikely, since they are not among the known targets of caspases (Casiano et al., 1996; Fischer et al., 2003). Actually, these precocious alterations are likely to precede the activation of effective caspases (Scovassi and Torriglia, 2003), since chromatin did not undergo significant structural changes and no DNA laddering, nor PARP-1 degradation were observed to occur (personal unpublished observation); nevertheless, the plasma membrane of treated cells showed typical early apoptotic features, such as the exposure of phosphatidylserine on the extracellular surface (Fadok et al., 1992; Martin et al., 1995).

At higher AMD concentrations (between 0.1 and 1 µg/ml), apoptosis massively occured with the typical morphological, cytochemical and cytometric evidence. Interestingly enough, residual extranucleolar RNA synthesis (demonstrated by BrU incorporation and the presence of DNA/RNA hybrid molecules) was still active in non-condensed chromatin, while apoptosis proceeds. Pre-mRNA maturation was, however, impaired since snRNP and the SC-35 splicing factor segregated from their usual nuclear locations, and entered the HERDS clusters, which passed into the cytoplasm prior to be released at the cell surface, inside apoptotic bodies. These structures have also been observed in different cell types where transcription was arrested, either physiologically or experimentally (Biggiogera et al., 1998, 2004; Biggiogera and Pellicciari, 2000). In our experiments, hnRNPs followed a different fate, and never participated in the formation of ectopic RNP aggregates.

We may conclude that the inhibition of r-RNA synthesis (with the consequent block in ribosome

production) and the defective pre-mRNA maturation seem to represent an early step of the AMD-induced apoptotic process: it may be hypothesized that these events may affect the equilibrium between transcription (still persisting until late apoptotic stages in the extranucleolar areas) and translation of some regulatory proteins required to maintain the control of the overall apoptotic machinery (Martin et al., 1990; Andera and Wasylyk, 1997; Peter et al., 1999).

Acknowledgements. This work was supported by the University of Pavia (Fondo di Ateneo per la Ricerca, FAR 2003). The authors wish to thank Ms. Paola Veneroni for her excellent technical assistance. Flow cytometric measurements were taken at the Centro Grandi Strumenti at the University of Pavia.

References

Andera L. and Wasylyk B. (1997). Transcription abnormalities potentiate apoptosis of normal human fibroblasts. Mol. Med. 12, 852-863.

Bernhard W. (1969). A new staining procedure for electron microscopical cytology. J. Ultrasruct. Res. 27, 250-255.

Biggiogera M. and Pellicciari C. (2000). Heterogeneous ectopic RNP-derived structures (HERDS) are markers of transcriptional arrest. FASEB J. 14, 828-834.

Biggiogera M., Bottone M.G. and Pellicciari C. (1998). Nuclear RNA is extruded from apoptotic cells. J. Histochem. Cytochem. 46, 988-1006.

Biggiogera M., Bottone M.G., Scovassi A.I. , Soldani C., Vecchio L. and Pellicciari C. (2004). Rearrangement of nuclear RNP-containing structures during apoptosis and transcriptional arrest. Biol. Cell 96, 603-615.

Caceres J.F., Misteli T., Screaton G.R., Spector D.L., Krainer A.L. (1997). Role of the modular domains of SR proteins in subnuclear localization and alternative splicing specificity. J. Cell Biol. 138, 225-238.

Casiano C.A., Martin S.J., Green R. and Tan E.M. (1996). Selective cleavage of nuclear autoantiges during CD95 (FAS/APO-1) mediated T cells apoptosis. J. Exp. Med. 184, 765-770.

Chen F.M. (1988). Binding specificities of actinomycin D to self-complementary tetranucleotide sequences -XGCY-. Biochemistry 27, 6393-6397.

Cmarko D., Verschure P., Martin T.E., Dahmus M.E., Krause S., Fu X.D., Van Driel R. and Fakan S. (1999). Ultrastructural analsis of transcription and splicing in the cell nucleus after BrUTP-microinjection. Mol. Biol. Cell 10, 211-223.

Dundr M. and Raska I. (1993). Nonisotopic ultrastructural mapping of transcription sites within the nucleolus. Exp. Cell Res. 208, 275-281

Fadok V.A., Voelker D.R., Campbell D.A., Cohen J.J., Bratton D.L. and Hensonp M. (1992). Exposure of phosphatidylserine on the surface of apoptotic lymphocytes triggers specific recognition and removal by macrophages. J. Immunol. 148, 2207-2216.

Fakan S. (1994). Perichromatin fibrils are in situ forms of nascent transcripts. Trends Cell Biol. 4, 86-90.

Fakan S. (2004). Ultrastructural cytochemical analyses of nuclear functional architecture. Eur. J. Histochem. 48, 5-14.

Fakan S., Leser G.P. and Martin T.E. (1986). Immunoelectron microscope visualization of nuclear ribonucleoprotein antigens within spread transcription complexes. J. Cell Biol. 103, 1153-1157.

Fischer U., Janicke R.U. and Schulze-Osthoff, K. (2003). Many cuts to ruin: a comprehensive update of caspase substrates. Cell Death Diff. 10, 76-100.

Fu X.D. and Maniatis T. (1992). The 35-kDa mammalian splicing factor SC35 mediates specific interactions between U1 and U2 small nuclear ribonucleoprotein particles at the 3' splice site. Proc. Natl. Acad. Sci. 89, 1725-1729.

Jensen P.O., Larsen J., Christiansen J. and Larsen J.K. (1993). Flow cytometric measurement of RNA synthesis using bromouridine labelling and bromodeoxyuridine antibodies. Cytometry 14, 455-458.

Jones R.E., Okamura C.S. and Martin T.E. (1980). Immunofluorescent localization of the protein of nuclear ribonucleoprotein complexes. J. Cell Biol. 86, 235-243.

Lerner E.A., Lerner M.R., Janeway C.A. and Steitz J. (1981). Monoclonal antibodies to nucleic acid-containing cellular constituents: probe for molecular and autoimmune disease. Proc. Natl. Acad. Sci. USA 78, 2737-2741.

Leser G.P., Escara-Wilke J. and Martin T.E. (1984). Monoclonal antibodies to heterogeneous nuclear RNA-protein complexes. J. Biol. Chem. 259, 1827-1833.

Martin S.J. (1993). Protein or RNA synthesis inhibition induces apoptosis of mature human CD4+ T cell blasts. Immunol. Lett. 35, 125-134.

Martin S.J., Lennon S.V., Bonham A.M. and Cotter T.G. (1990). Induction of apoptosis (programmed cell death) in human leukemic HL-60 cells by inhibition of RNA or protein synthesis. J. Immunol. 145, 1859-1867.

Martin S.J., Reutlingspenger C.P.M., Mc Gohon A.J., Rader J., Van Schil R.C.A.A., La Face D.M. and Green D.R. (1995). Early redistribution of plasma membrane phosphatidylserine is a general feature of apoptosis regardless of the initiating stimulus: inhibition by overexpression of Bcl-2 and Abl. J. Exp. Med. 182, 1-12.

Martin T.E. and Okamura C.S. (1981). Immunocytochemistry of nuclear hnRNP complexes. In: The cell nucleus. Vol. 9. Busch H. (ed). Academic Press. New York. pp 119-144.

Melcak I., Cermanova S., Jirsova K., Koberna K., Malinsky J. and Raska I. (2000) Nuclear pre-mRNA compartmentalization: trafficking of released transcripts to splicing factor reservoirs. Mol. Biol. Cell. 11, 497-510.

Melcak I., Melcakova S., Kopsky V., Vecerova J. and Raska I. (2001). Prespliceosomal assembly on microinjected precursor mRNA takes place in nuclear speckles. Mol. Biol. Cell. 12, 393-406.

Misteli T. and Spector D.L. (1997). Protein phosphorylation and the nuclear organization of pre-m RNA splicing. Trends Cell Biol. 7, 135-138.

Misteli T. and Spector D.L. (1998). The cellular organization of gene expression. Curr. Opin. Cell Biol. 10, 323-331.

Naora H., Nishida T., Shindo Y., Aadachi M. and Naora H. (1996). Constitutively enhanced nbl expression is associated with the induction of internucleosomal DNA cleavage by actinonycin D. Biochem. Biophys. Res. Commun. 224, 258-264.

Pellicciari C., Manfredi A.A., Bottone M.G., Schaack V. and Barni S. (1993). A single-step staining procedure for the detection and sorting of unfixed apoptotic thymocites. Eur. J. Histochem. 37, 381-390.

Pellicciari C., Bottone M.G. and Biggiogera M. (1997). Detection of apoptotic cells by Annexin V labelling at electron microscope. Eur. J. Histochem. 41, 211-216.

Perry R.P. and Kelley D.E. (1968). Persistent synthesis of 5S RNA when production of 28S and 18S ribosomal RNA is inhibited by low doses of actinoycin D. J. Cell Physiol. 72, 235-246.

Perry R.P. and Kelley D.E. (1970). Inhibition of RNA synthesis by actinomycin D: characteristic dose-response of different RNA species. J. Cell Physiol. 76, 127-139.

Peter M.E., Scaffidi C., Medema J.P., Kischkel F. and Krammer P.H. (1999). The death receptors. In: Apoptosis: Biology and mechanism". Spriger-Verlag. Berlin, pp.25-63.

Puvion E. and Puvion-Dutilleul F. (1996). Ultrastructure of the nucleus in relation to transcription and splicing: roles of perichromatin fibrils and interchromatin granules. Exp. Cell Res. 229, 217-225.

Puvion-Dutilleul F., Mazan S., Nicoloso M., Pichard E., Bachellerie J.P. and Puvion E. (1992). Alterations of nucleolar ultrasructure and ribosome biogenesis by actiomycin D. Implications for U3 snRNP function. Eur. J. Cell Biol. 58, 149-162.

Scovassi A.I. and Torriglia A. (2003). Activation of DNA-degrading enzymes during apoptosis. Eur. J. Histochem. 47, 185-194.

Shah G.M., Poirier D., Duchaine C., Brochu G., Desnoyers S., Lagueux J., Verreault A., Hoflack J.C., Kirkland J.B. and Poirier G.G. (1995). Methods for biochemical study of poly(ADP-ribose) metabolism in vitro and in vivo. Anal. Biochem. 227, 1-13.

Spector D.L. (1996). Nuclear organization and gene expression. Exp. Cell Res. 229, 189-197.

Spector D.L., Fu X.D. and Maniatis T. (1991). Associations between distinct pre-mRNA splicing components and the cell nucleus. EMBO J. 10, 3467-3481.

Testillano P.S., Gorab E. and Risueño M.C. (1994). A new approach to map transcription sites at the ultrastructural level. J. Histochem. Cytochem. 42, 1-10.

Wansink D.G., Nelissen R.L. and de Jong L. (1994). In vitro splicing of pre-m RNA containing bromouridine. Mol. Biol. Rep. 19, 109-113.

Accepted September 13, 2004